

Low dark current and Type-II band Alignment in Double Perovskite Single Crystal $\text{Cs}_2\text{AgBiBr}_6$ / $\text{Cs}_3\text{Bi}_2\text{I}_9$ Nanocrystals Heterojunction Enables High-Performance Photodetection

Ravinder Chahal¹, Koushik Ghosh¹, Shipra Aswal² Joydip Ghosh³, P. K. Giri^{1,2*}

¹Department of Physics, Indian Institute of Technology Guwahati, Guwahati, India, 781039

²Centre for Nanotechnology, Indian Institute of Technology Guwahati, Guwahati, India, 781039

³Inorganic Chemistry Laboratory, University of Oxford, Oxford OX1 3QR, United Kingdom

ravinder19@iitg.ac.in, g.koushik@iitg.ac.in, shipra@iitg.ac.in, jghosh2010@gmail.com,
giri@iitg.ac.in

*Corresponding author, Email: giri@iitg.ac.in

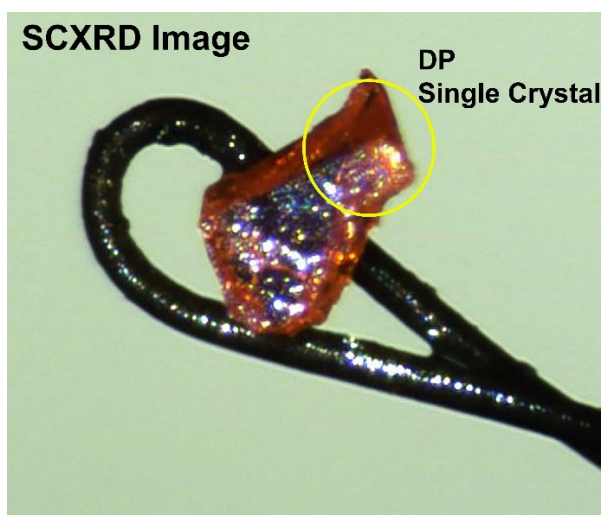


Fig. S1: Optical image of the DP single crystal mounted on the nylon loop with the help of silicon oil for SCXRD measurement.

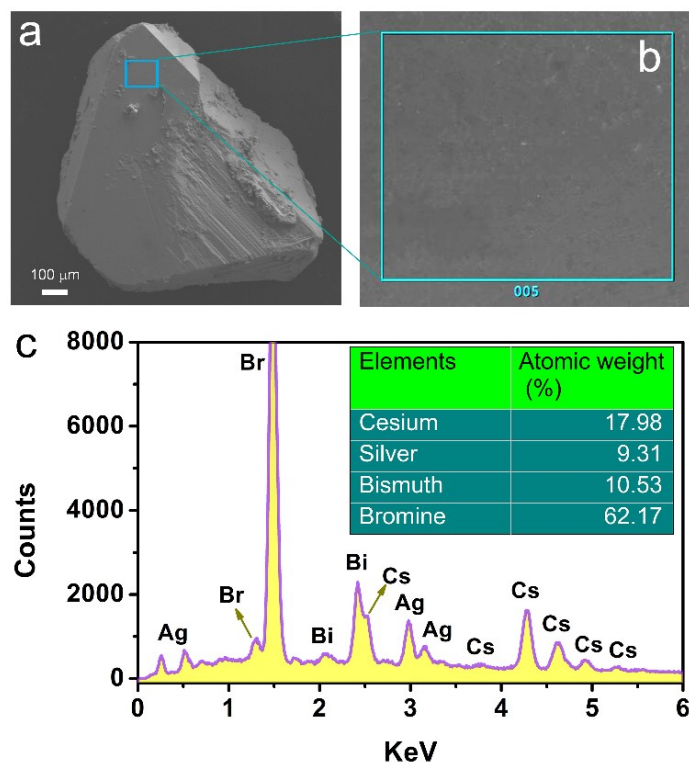


Fig. S2: (a) FESEM image of the $\text{Cs}_2\text{AgBiBr}_6$ single crystal. (b) Magnified FESEM image of the marked area of $\text{Cs}_2\text{AgBiBr}_6$ single crystal. (c) Corresponding FESEM-EDX atomic spectra of $\text{Cs}_2\text{AgBiBr}_6$ single crystal. The inset shows the corresponding atomic percentage of each element.

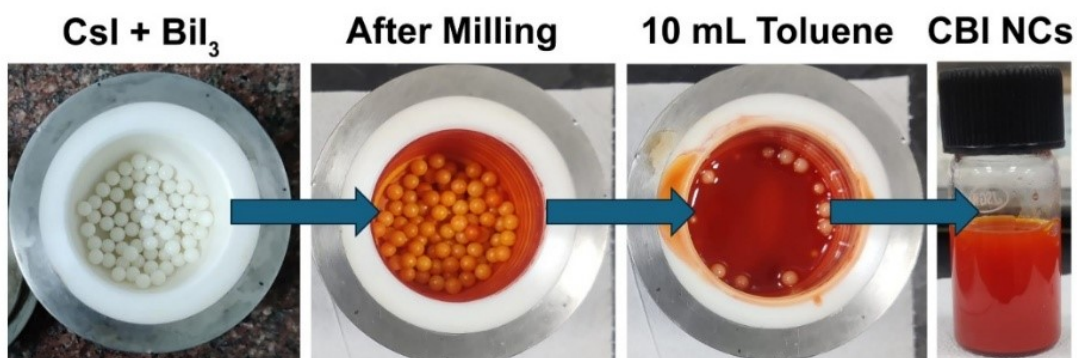


Fig. S3: Schematic illustration of the preparation method of $\text{Cs}_3\text{Bi}_2\text{I}_9$ NCs using the ball milling method.

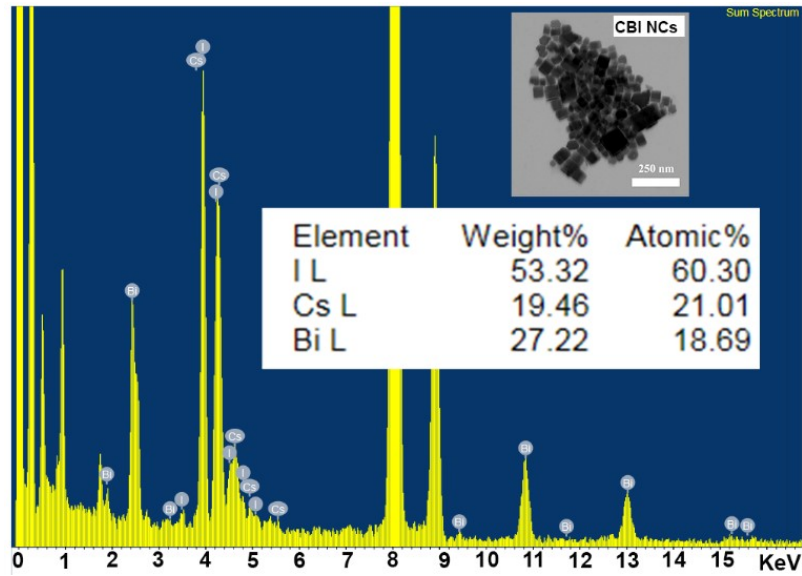


Fig. S4: FETEM-EDX atomic spectra of $\text{Cs}_3\text{Bi}_2\text{I}_9$ NCs.

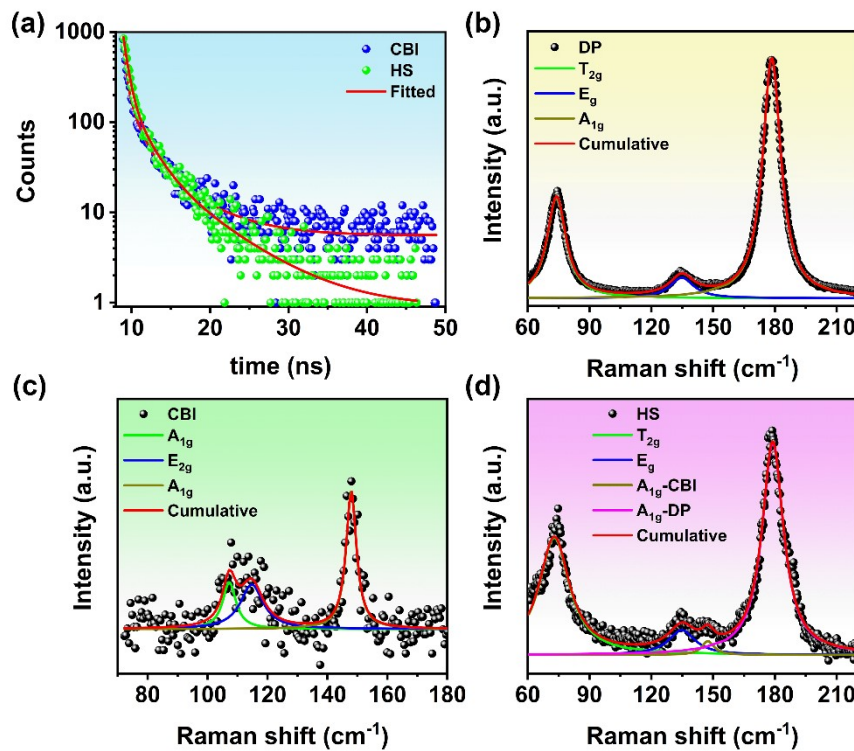


Fig. S5: (a) TRPL spectra of $\text{Cs}_3\text{Bi}_2\text{I}_9$ and $\text{Cs}_2\text{AgBiBr}_6/\text{Cs}_3\text{Bi}_2\text{I}_9$ HS. Deconvoluted Raman spectra of (b) $\text{Cs}_2\text{AgBiBr}_6$ SC, (c) $\text{Cs}_3\text{Bi}_2\text{I}_9$ NC thin film, and (d) $\text{Cs}_2\text{AgBiBr}_6/\text{Cs}_3\text{Bi}_2\text{I}_9$ heterostructure.

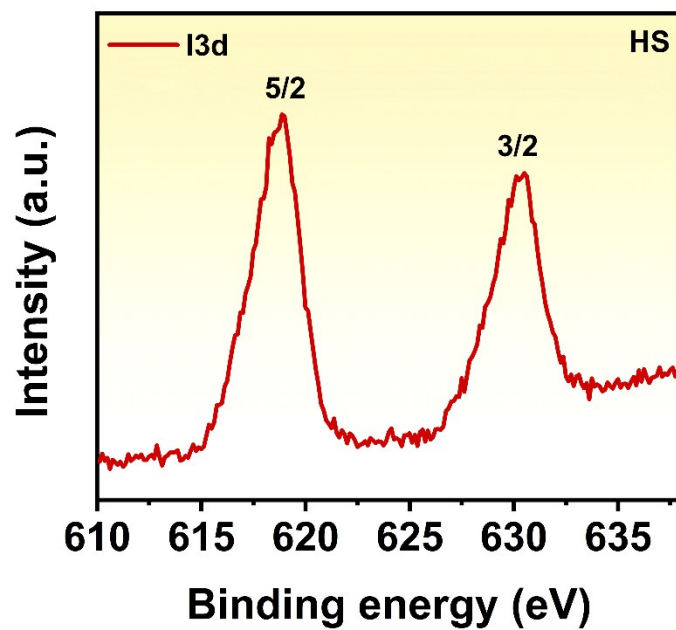


Fig. S6: XPS spectra of Iodine in the DPSC/CBI HS system.

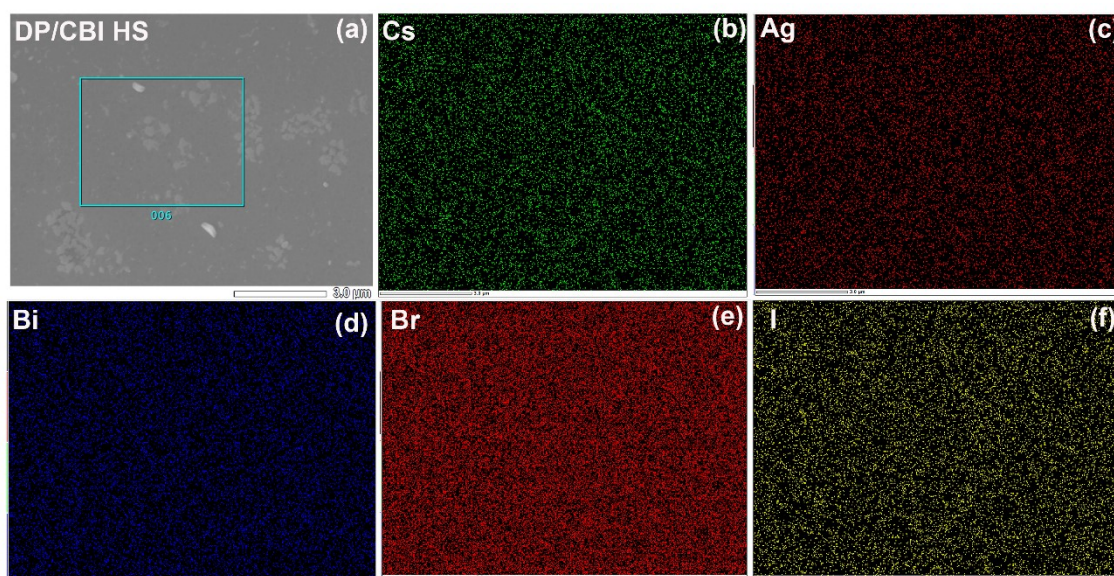


Fig. S7: (a) FESEM image of the DP/CBI HS. (b-f) FESEM-EDX mapping of all the constituent elements present in the HS.

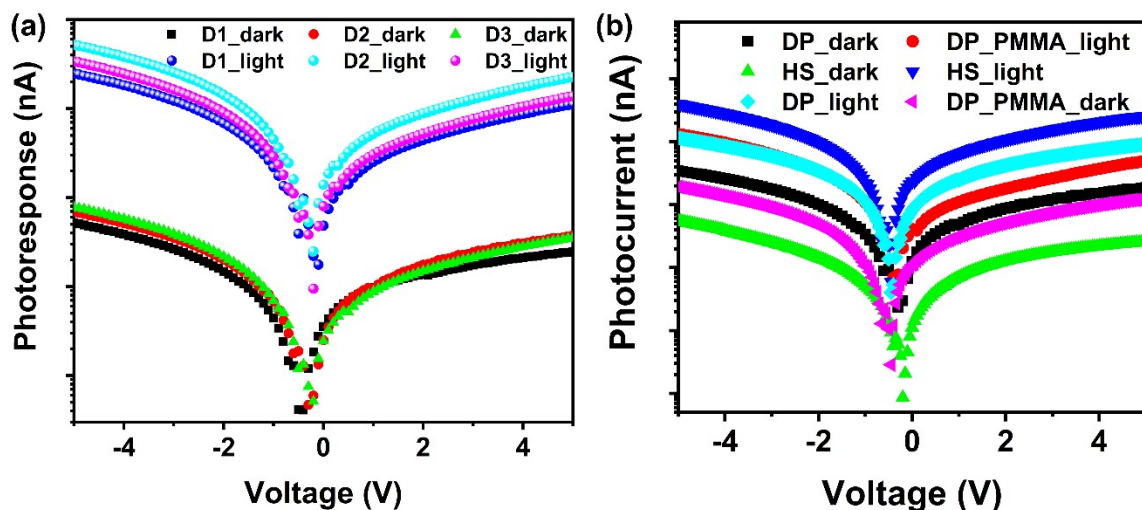


Fig. S8: (a) I-V characteristics of the multiple HS devices with the same configuration. (b) Comparison of the I-V characteristics of DP, DP-PMMA, and HS devices.

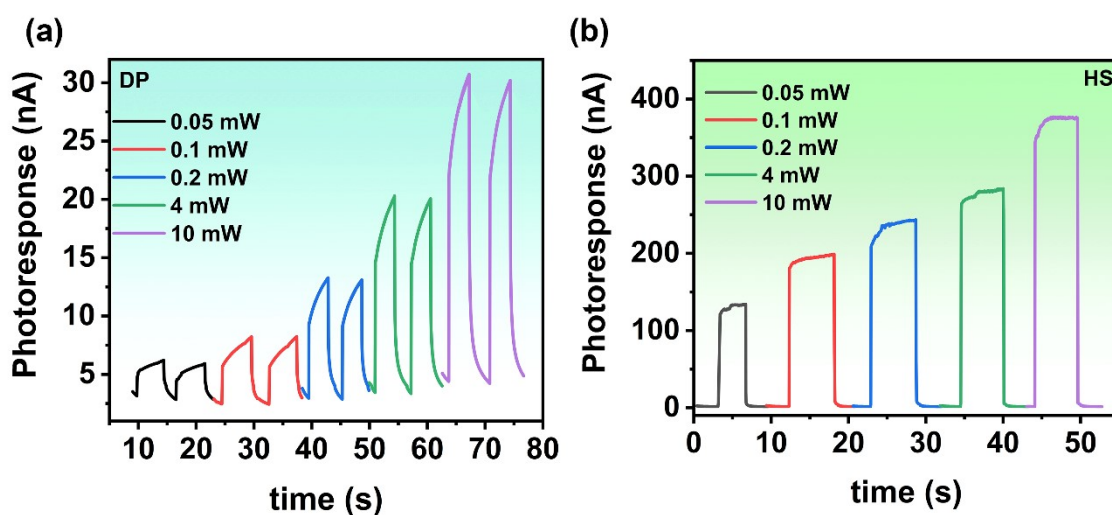


Fig. S9: Power-dependent photoresponse of the pristine and HS device under 450 nm laser illumination.

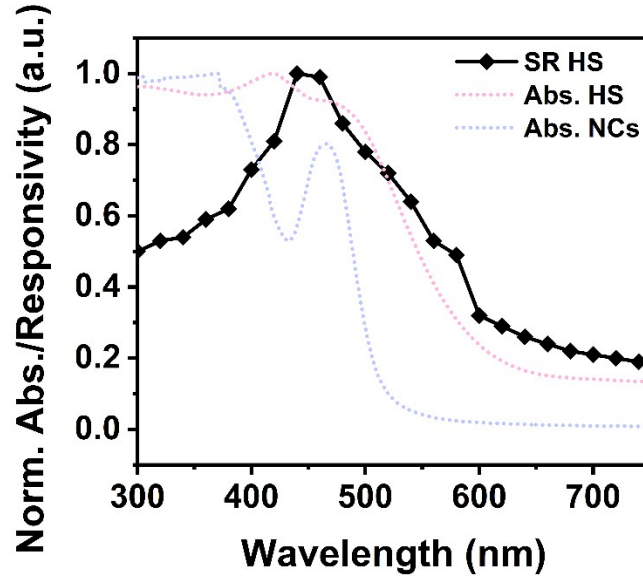


Fig. S10: Spectral responsivity of the HS device with reference to the absorbance of HS and CBI NCs.

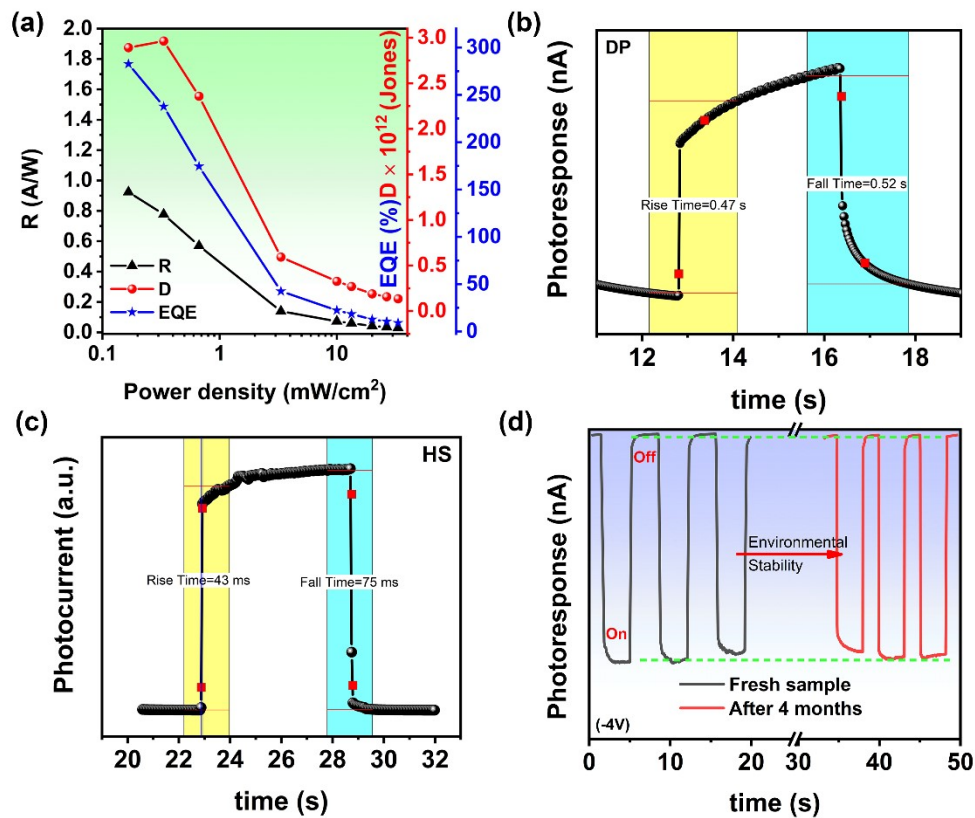


Fig. S11: (a) Comparison of responsivity, detectivity and external quantum efficiency of the $\text{Cs}_2\text{AgBiBr}_6/\text{Cs}_3\text{Bi}_2\text{I}_9$ heterostructure device. (b, c) rise and fall time of pristine $\text{Cs}_2\text{AgBiBr}_6$ SC and $\text{Cs}_2\text{AgBiBr}_6/\text{Cs}_3\text{Bi}_2\text{I}_9$ heterostructure device. (d) Stability performance of the HS device after 4 months of storage under ambient conditions.

Table S1: The unit cell parameters obtained from SCXRD measurement.

Parameters	Compound name
Formula	Ag ₂ Bi ₂ Br ₁₂ Cs ₄
Mol.wt.	2124.26
Crystal System	Cubic
Space group	Fm-3m
a (Å)	11.264(6)
b (Å)	11.264(6)
c (Å)	11.264(6)
α (°)	90
β (°)	90
γ (°)	90
V (Å ³)	1429.3(2)
Density, gcm ⁻³	4.936
Abs. coeff., mm ⁻¹	35.408
F (000)	1800
Total no. of reflections	110
Reflections, I > 2 σ (I)	110
Max. θ /°	25.242
Ranges (h, k, l)	-14 ≤ h ≤ 14 -14 ≤ k ≤ 14 -14 ≤ l ≤ 14
Complete to 2 θ (%)	98.9
Data / restraints / parameters	110/0/8
GooF (F ²)	1.265
R indices [I > 2 σ (I)]	0.0112
wR ₂ [I > 2 σ (I)]	0.0258
R indices (all data)	0.0112
wR ₂ (all data)	0.0258

Table S2: Peak positions of A_{1g} Raman mode in pristine and the HS materials obtained from the fitted Raman spectra in Fig. S5.

Material	A _{1g} -mode (peak position) (cm ⁻¹)
Cs ₂ AgBiBr ₆ (DP)	178.93
Cs ₃ Bi ₂ I ₉ (CBI)	147.44
Cs ₂ AgBiBr ₆ /Cs ₃ Bi ₂ I ₉ HS	DP (A _{1g}) - 178.45 CBI (A _{1g}) - 147.93

Table S3: Stoichiometric ratio calculations obtained from deconvoluted XPS spectra of each element.

Element	Peak Area (A)	RSF (S)	Corrected Intensity (A/S)	Atomic %	Stoichiometric Ratio (Bi=1)
Cs	60835.42	7.041	8640.17	27.8	2.67
Ag	15819.38	5.987	2642.29	8.5	0.82
Bi	29549.46	9.140	3232.98	10.4	1.00
Br	14966.11	1.053	14212.83	45.7	4.40
I	14777.52	6.206	2381.17	7.7	0.74

Table S4: Comparison of the theoretical and measured composition of the DPSC/CBI HS from XPS data.

Composition	Cs	Ag	Bi	Br	I	Comment
Ideal Cs₂AgBiBr₆	2	1	1	6	0	No Iodide
Ideal Cs₃Bi₂I₉	1.50	0	1	0	4.50	No Silver, No Bromide
Theoretical (90:10) (Cs₂AgBiBr₆:Cs₃Bi₂I₉)	1.91	0.82	1	4.91	0.82	Expected for 90:10 mixture for Bi=1
XPS (Bi=1)	2.67	0.82	1	4.40	0.74	Measured surface composition